Green Decomposition of Organic Dyes Using Octahedral Molecular Sieve Manganese Oxide Catalysts

Thamayanthy Sriskandakumar,[†] **Naftali Opembe,**[†] **Chun-Hu Chen,**[†] **Aimee Morey,**[†] **Cecil King'ondu,**[†] **and Steven L. Suib***[,†,‡]

Department of Chemistry, University of Connecticut, 55 North Eagleville Road, Storrs, 06269-3060, U.S.A.

Received: August 27, 2008; Revised Manuscript Received: December 16, 2008

The catalytic degradation of organic dye (methylene blue, MB) has been studied using green oxidation methods (tertiary-butyl hydrogen peroxide, TBHP, as the oxidant with several doped mixed-valent and regular manganese oxide catalysts in water) at room and higher temperatures. These catalysts belong to a class of porous manganese oxides known as octahedral molecular sieves (OMS). The most active catalysts were those of Mo^{6+}- and V^{5+}-doped OMS. Rates of reaction were found to be first-order with respect to the dye. TBHP has been found to enhance the MB decomposition, whereas H_2O_2 does not. Reactions were studied at pH 3−11. The optimum pH for these reactions was pH 3. Dye-decomposing activity was proportional to the amount of catalyst used, and a significant increase in catalytic activity was observed with increasing temperature. X-ray diffraction (XRD), energy dispersive spectroscopy (EDX), and thermogravimetric analysis (TGA) studies showed that no changes in the catalyst structure occurred after the dye-degradation reaction. The products as analyzed by electrospray ionization mass spectrometry (ESI-MS) showed that MB was successively decomposed through different intermediate species.

Introduction

Today more than 100 000 commercially available organic dyes play a major role in not only the traditional textile and dyeing industries but also in new areas such as food, pharmaceutical, cosmetics, imaging biological samples, liquid crystals, lasers, solar cells, as well as optical data discs and computer industries. These newly developed applications are based on color changes but pose pollution problems in the form of colored wastewater being discharged into water bodies. Discharging most of these dyes creates acute problems to the ecosystem as they are microtoxic, mutagenic, and carcinogenic for aquatic life as well as humans. Therefore, the removal of dyes from waste effluents has become environmentally important because contamination of dyes even at 1.0 mg/L results in water that is unfit for human consumption.[1−6]

Globally, there has been a growing interest in the development of advanced oxidation processes for dye removal from water streams. Breaking bonds in the dye molecules is sufficient to remove unwanted color but products created during oxidation are sometimes difficult to convert into harmless small fragments (CO_2 and H_2O).[7] The goal of the oxidation process is to decompose the carbon and hydrogen atoms of the dye to carbon dioxide and water. Several oxidation methods have been reported with the combined effect of hydrogen peroxide (oxidant) and metal oxides.[8−10]

Manganese oxides are one of the largest families of porous materials with various structures. Among these, tunnel structure octahedral molecular sieves (OMS), octahedral layered structure (OL-1), and amorphous manganese oxide (AMO) materials have been extensively studied in our laboratory.[11−16] OMS-2, shown in Figure 1, the main catalyst used in this work, is a microporous
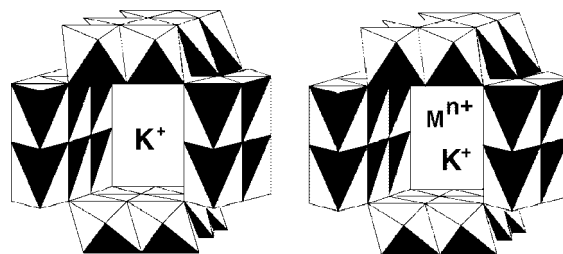

Figure 1. Structures of K−OMS-2 and doped K−OMS-2 catalysts.

(diameters of pores ∼4.5 to 6.5 Å),[17] tunnel-structured (4.6 × 4.6 Å² tunnels in 2 × 2 arrangement), and mixed-valent (the average manganese oxidation state is 3.9 in the presence of a mixture of Mn^{4+}, Mn^{3+}, and Mn^{2+} ions) material with a Lewis acidity of 0.7 and basicity of 0.05.[18−21] OMS-2 is a very good oxidation catalyst for organic species due to high specific surface area, high porosity, and average oxidation state.

Catalytic applications of these materials showed that various organic molecules and functional groups are effectively oxidized in the presence of OMS-2 such as: partial oxidation of butane[22] and cycloalkanes,[23] oxidation of alcohols,[24] indene,[18,25] 9H-fluorene,[26] conversion of ethylbenzene to styrene,[27] conversion of *n*-paraffin to *n*-olefin, oxidative dehydrogenation of cyclohexane,[28] partial epoxidation of olefins[29] and epoxidation of styrene,[21] syntheses; of 2-aminodiphenylamine,[30] imines,[31] and 2-thiophenemethanol.[32] These reactions show the ability of OMS to react with organic substrates, which contain different heteroatoms − nitrogen and sulfur and also carbon. In addition, OMS-2 and doped OMS-2 materials were successfully used to decompose the pinacyanol chloride (PC), cyanine dye in our laboratory.[10]

The current study reports a green decomposition of methylene blue (MB) (Figure 2), the most important basic cationic dye, using *tert*-butyl hydroperoxide (TBHP) as the oxidant with the catalysts of OMS-2 and doped OMS-2 materials as catalysts in

* To whom correspondence should be addressed. E-mail: steven.suib@uconn.edu. Phone: 860-486 2797. Fax: 860-486 2981.
† Department of Chemistry.
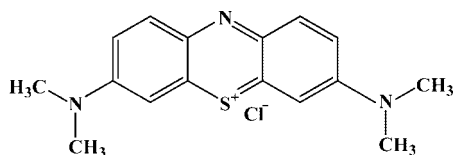‡ Institute of Material Science.

Figure 2. Structure of MB dye.

aqueous media. This heterogeneous catalysis method, because of its nature, seems to be the most economically attractive and environmentally friendly oxidation technology for the treatment of organic pollutants. To our knowledge, this is the first report investigating TBHP as an oxidant for MB decomposition with OMS-2 catalysts.

The extent of dye decomposition was monitored using UV−vis spectroscopic techniques. The effects of TBHP concentration and of doped metals have been studied and the kinetics of these reactions investigated. In addition, parameters such as catalyst amount, pH, and temperature on the rate of MB decomposition were examined. XRD was used to confirm the crystalline structure of the catalysts before and after the catalytic reaction. Finally, ESI-MS experiments were performed to analyze the products of this reaction.

Experimental Section

Reagents. The basic cationic dye methylene blue (MB) was purchased from Pfalz&Bauer Inc. (Flushing, NY) and was used without further purification. MB exhibits a maximum absorbance (λ_{max}) at 665 nm and is dark blue in color. *tert*-Butyl hydroperoxide (TBHP, 70% in water) was from Sigma Aldrich, Inc. (St. Louis, MO) and hydrogen peroxide (30%) was obtained from Fischer Scientific (Fair City Lawn, NJ). Dye and peroxide solutions were made fresh in distilled deionized water (DDW) just before the experiment. All of the other chemicals were of analytical grade and were purchased from Aldrich.

Synthesis of Catalysts. Doped and undoped OMS-2, having the cryptomelane structure, were prepared by refluxing mixtures of $KMnO_4$, $MnSO_4$, concentrated HNO_3 and corresponding metal nitrates or oxides in aqueous solution for 24 h.[18] H−K−OMS-2 and Nano-K−OMS-2 were prepared according to the procedures used by Makwana et al.[33] and Villegas et al.,[16] respectively. OMS-1, todorokite, was synthesized using a precipitation method by adding the mixture of NaOH, $MgCl_2$, and $MnSO_4$ to a solution of $KMnO_4$.[34] OL-1, birnessite, was prepared following our previous report.[35] Amorphous manganese oxides (AMO) were prepared by reduction of $KMnO_4$ with oxalic acid following the procedure described elsewhere.[10] Commercial MnO_2 (pyrolusite) was obtained from Johnson Matthey, Inc. Seabrook, NH.

MB Decomposition. The catalysts to be tested were dried overnight at 110 °C (to remove moisture) prior to the catalytic reactions. The catalytic reaction was carried out in a 250 mL batch reactor at room temperature by mixing 50 mL each of dye and peroxide. After adding 50 mg of catalyst, the flask was sealed and allowed to react for 120 min with continuous stirring. The concentrations of reactants in the reactor were 5×10^{-4} M in TBHP (or H_2O_2) and 60 ppm (1.6×10^{-4} M) in the dye. Reactions were also performed in the absence of oxidant by substituting DDW for TBHP and allowed to react for 30 min. The effects of oxidant and catalyst concentrations were studied by changing the TBHP concentration from 5×10^{-6} to 5×10^{-4} M and the catalyst amount from 12.5 to 100.0 mg, respectively. A pH range of 3−11 was used to study the reaction by using buffers made of acetate, carbonate, borate, and

phosphate salts. The initial pH was adjusted with 4.0 M NaOH or HCl solution using an Oakton pH meter equipped with a combined pH electrode. The pH meter was calibrated using standard buffer solutions purchased from Sigma before every measurement. Dye-decomposition studies were also carried out at different temperatures from 20.0 to 80.0 °C (±0.5 °C) using an oil bath to keep the temperature constant, and a condenser to avoid the solution being evaporated at higher temperature. All of the experiments were carried out in duplicate.

Optical absorbance measurements were taken by pipetting 0.5 mL aliquots of the reaction mixture at various time intervals during the reaction, and quickly diluting with water to 5 mL prior to analysis. The diluted solution was immediately centrifuged for 5 min at 8000 rpm to remove any solid particulates, which tend to scatter the incident beam. The centrifuged solution was then put into a quartz cell of path length 1.0 cm, and the absorbance spectrum was measured using a Hewlett-Packard 8453 diode array UV−vis spectrophotometer. A linear calibration curve for the dye concentrations was obtained by monitoring the peak intensity (λ_{max}) at 665 nm for a series of standard solutions according to Beer's law. To avoid constructing calibration curves of MB for each pH value, the % decrease of MB is calculated using eq 1,[36]

$$\% \text{ decrease in MB} = \left(\frac{A_0 - A_t}{A_0} \right) \times 100\% \qquad (1)$$

where A_0 and A_t are absorbance at 0 min and at a given time respectively, and those values correspond to the initial and final dye concentrations in the reaction mixture at a given pH value.

Catalyst Structure and Surface Area Determination. X-ray diffraction analysis was performed on the catalysts using a Scintag model PDS-2000 $\theta\theta$ diffractometer, before and after the reaction to see if any structural changes occurred during the reaction. The surface area of the materials was measured using the Braunner-Emmet-Teller (BET) method on a Micromeritics ASAP 2010 instrument. Analysis was made by a multipoint method with N_2 gas as the absorbent.

Potentiometric Titrations, Chemical Composition and Thermal Stability Analysis. The average oxidation state (AOS) was determined by performing potentiometric titrations.[16] Chemical composition and thermal stability of K−OMS-2 catalysts were determined before and after the reaction to see if any structural changes occurred during the reaction. Briefly, thermogravimetric analysis was performed on a TA Instruments TGA 2950. The program was run from about 25 °C (room temperature) to 900 °C at a ramp rate of 10 °C per minute under an argon atmosphere, elemental composition was performed on an Amray 1810 D instrument, with an Elemental analysis obtained from K K-alpha, Mn K-alpha, calculated for pure elements on a IXRF Systems 500 digital processor at 15 kV accelerating potential.

Product Analysis. To identify the intermediates formed from the MB decomposition, the product analysis was performed with the positive ion mode ESI-MS of a Micromass Quattro II, Beverly, MA, mass spectrometer. The reaction samples, removed at different time intervals during the reaction, were analyzed by introducing the aliquots into the ESI source. Typical ESI conditions were heated capillary temperature 150 °C, sheath gas N_2 at a flow rate of 20 units, cone voltage of 30 V, and capillary voltage of 3.5 eV.

Results

Effect of Oxidants. Part b of Figure 3, a plot of percentage decrease in [MB] versus time, represents the influence of oxidant
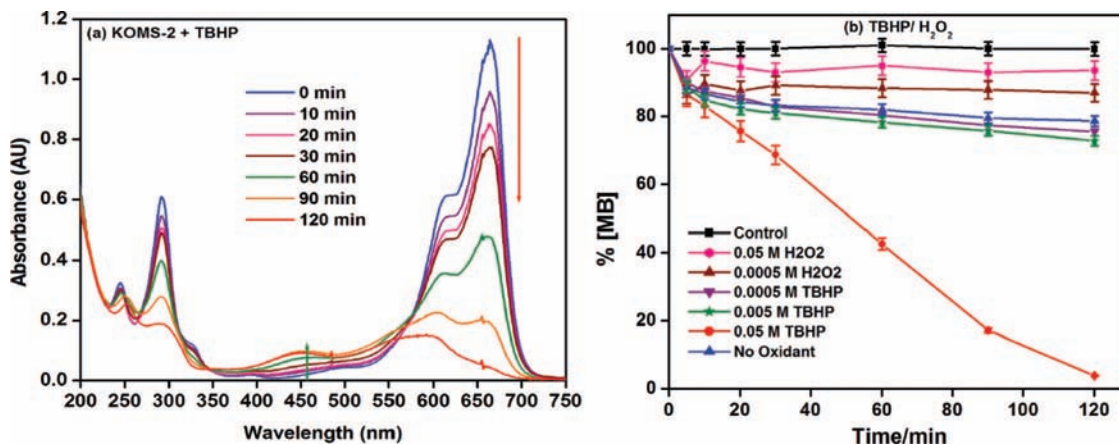
Figure 3. (a) Changes in the UV−vis absorbance spectra of MB dye using K−OMS-2 with TBHP for 120 min. Fifty milliliters of 120 ppm dye was reacted with 50 mL of 0.1 M TBHP and 50 mg of K−OMS-2 at 20 °C. (b) Percentage decomposition of MB with varying concentrations of TBHP/H2O2.

(TBHP/H_2O_2) on the decomposition of MB dye catalyzed by OMS-2 catalysts at room temperature. Blank reactions (control) were first done at room temperature in the presence of oxidants (50 mL of TBHP/ H_2O_2 + 50 mL of 120 ppm MB dye) but without any catalysts in which no dye decomposition was observed even after 120 min. The activity of the catalysts is expressed as the percent decrease in dye concentration during the reaction. This quantity is proportional to the color loss of the dye during the reaction.

Experiments were then carried out by varying the initial TBHP/H_2O_2 concentrations with catalysts present. Part b of Figure 3 shows the results of these experiments. In experiments where no oxidant was used, the concentration of dye was only reduced by between 25−30% in 30 min and then tended to remain constant. However, when the initial [TBHP] was increased, a drastic increase (from 20% to 95%) in dye decomposing activity was observed. A complete decolorization was observed in the presence of 0.05 M TBHP after 120 min reaction. Whereas when the initial [H_2O_2] was increased, a decrease (from 20% to 6%) in the decomposition was observed. This suggests that TBHP induces the catalytic ability of OMS-2 materials to degrade MB, whereas H_2O_2 inhibits such ability of these materials. Therefore, TBHP is a better oxidant for K−OMS-2 catalyst, and 0.05 M is its critical concentration for these experiments. Part a of Figure 3 shows a steady decrease of the absorbance of the dye occuring in the UV−vis spectra with the progress of the reaction when K−OMS-2 catalyst was used with 0.05 M TBHP.

Doped Catalysts' Effect. To study the effect of doped K−OMS-2 catalysts on dye decomposition, catalytic reactions were carried out with selected doped (H, V, Fe, Mo, W, and Co) OMS-2 catalysts for 30 min, and the result is tabulated in Table 1 (column 2). Part b of Figure 4 shows the trend and degree of MB decomposition catalyzed by H-, V-, and Mo-doped OMS-2 catalysts compared to regular K−OMS-2. OMS-2 materials doped with V (75% decrease in MB) and Mo (94% decrease in MB) show a high impact on catalytic activity, whereas other doped (H, Fe, W, and Co) materials showed less activity than undoped K−OMS-2 material. Part a of Figure 4 shows the UV−vis absorbance spectrum with time when Mo−K−OMS-2 was used as catalyst. These results indicate that addition of dopants causes changes in the ability of catalysts to decompose the dye.

Combined Effects of Doped Catalyst and TBHP. Table 1 describes the combined effect of doped catalysts and TBHP on

TABLE 1: BET Surface Area and Dye Decomposition Activities of Various Doped K−OMS-2 Catalysts with[b] and without[a] TBHP

catalyst	[a] % dec_{30}[c]	[b] % dec_{120} with TBHP[d]	BET surface area (m²/g)
K−OMS-2	28	96	88
H−K−OMS-2	21	76	63
V−K−OMS-2	75	88	179
Fe−K−OMS-2	17	61	160
Mo−K−OMS-2	94	98	270
W−K−OMS-2	20	84	64
Co−K−OMS-2	16	29	19

[a] Reaction Conditions: 25 mL of 120 ppm MB dye, 75 mL of DDW, 50 mg of catalyst. [b] Reaction Condition: 50 mL of 120 ppm MB dye, 50 mL of 0.1 M TBHP, 50 mg of catalyst. [c] Percent decrease in [MB] after 30 min of reaction. [d] Percent decrease in [MB] after 120 min of reaction.

the MB decomposition along with the surface areas of the catalysts. TBHP gives enhancement effects (29−98%) with doped catalysts as with undoped catalysts. UV−vis spectrum (Figure S1 of the Supporting Information) of the reaction in the presence of Mo−K−OMS-2 with TBHP shows that the dye is fully removed after 120 min and the spectrum at this time looks close to a blank solution, DDW.

Kinetic Studies. Kinetics of MB decomposition reactions were studied by considering two typical reactions where MB was completely decomposed with Mo−K−OMS-2 as catalyst and K−OMS-2 catalyst used along with TBHP. Part a of Figure 5 illustrates, with an assumption of first-order kinetics, a plot of ln ([MB]$_0$/[MB]) versus time for the MB decomposition reaction where Mo−K−OMS-2 was used as catalyst. The data, taken during the course of a 30 min reaction period, show a good linear correlation (R^2 = 0.9989), suggesting that the reaction follows first-order kinetics with respect to the dye. The slope of the linear line reveals a first-order rate constant, k = 7.6 × 10^{-2} min^{-1}. The plots of zero-order and second-order kinetics gave poor linear correlation (R^2) values.

With the same assumption, a plot of ln ([MB]$_0$/[MB]) versus time was made and is represented in part b of Figure 5 for the dye decomposition of K−OMS-2 with 0.05 M TBHP over a time of 120 min. The slope gives a good linear correlation (R^2 = 0.9983) suggesting that the reaction follows a pseudo-first-order rate law with respect to dye concentration. The rate constant of the reaction from the slope, and k is equal to 3.7 × 10^{-2} min^{-1}. Kinetic data obtained for these two reactions were
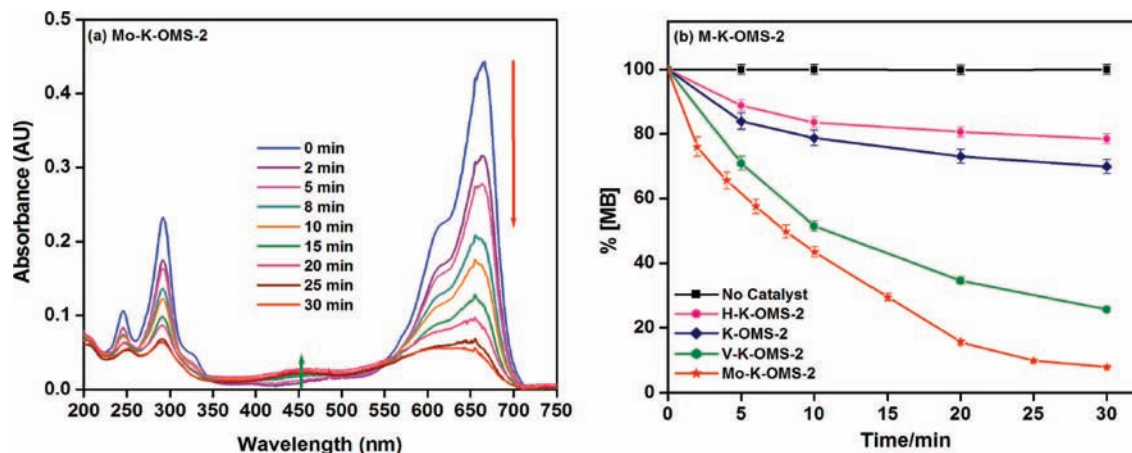
Figure 4. (a) Changes in the UV–vis absorbance spectra of MB dye using Mo–K–OMS-2 for 30 min. A 25 mL of 120 ppm dye + 75 mL of DDW was reacted with 50 mg of Mo–K–OMS-2 at 20 °C. (b) Decomposition of MB using different doped K–OMS-2 catalysts under the same conditions.
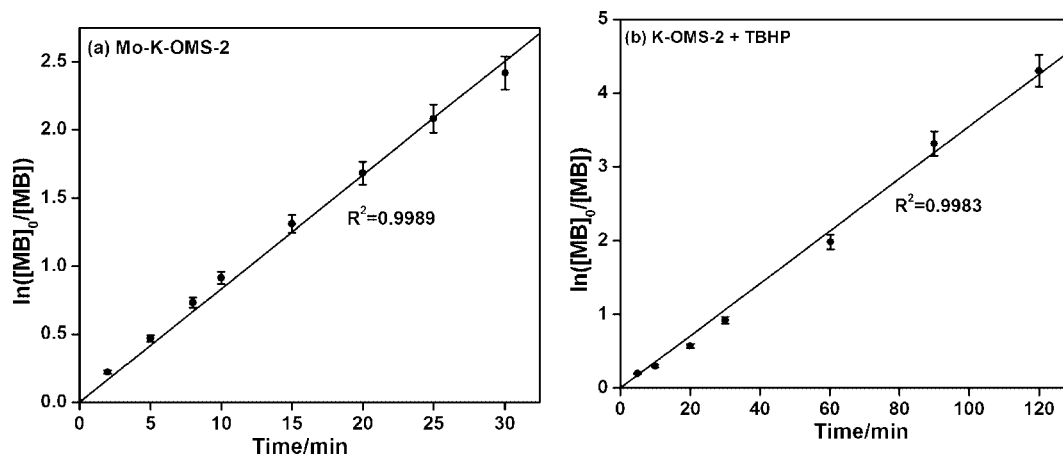

Figure 5. (a) First-order kinetic plot of ln[MB] vs time of a 25 mL of 120 ppm dye + 75 mL of DDW was treated with 50 mg of Mo–K–OMS-2 at 20 °C for 30 min. (b) Pseudo-first-order kinetic plot of ln[MB] vs time of a 50 mL of 120 ppm dye was reacted with 50 mL of 0.1 M TBHP + 50 mg of K–OMS-2 at 20 °C for 120 min. Error bar was made for three repeated trials of each time point. Solid line is the best fit of the slope.

also fit to higher-order (second and third) kinetics and resulted in lower R^2 values implying poor correlation.

Temperature Effect. A series of similar experiments were conducted at temperatures of 20, 40, 60, and 80 °C to study the effect of dye decomposition by K–OMS-2 with and without TBHP and Mo–K–OMS-2. This is illustrated in part a of Figure 6. A general trend of an increase in MB decomposition with increasing temperature was observed in all three cases. However, a drastic but steady increase in reaction activity was observed with temperature when TBHP was used with K–OMS-2 catalyst. Because of this increased activity at higher temperatures, the dye decomposition was complete in 10 min at 80 °C as compared to 2 h at room temperature. Doped Mo–K–OMS-2 catalyst shows a sudden increase at 40 °C and then slightly increased at higher temperatures.

Because a steady increase on MB decomposition was observed for the K–OMS-2 + TBHP system, kinetics of that reaction was studied for different temperatures (part b of Figure 6), and then the pseudo-first-order rate constants were calculated from the slopes. The natural logarithm of the Arrhenius eq 2 is used to calculate the activation energy (E_a) of the reaction.

$$\ln k = -\frac{E_a}{R}\frac{1}{T} + \ln A \qquad (2)$$

k is the rate constant, E_a is the activation energy, R is the universal gas constant (8.314×10^{-3} kJmol^{-1}K^{-1}), and A is a

constant. Figure S2 in the Supporting Information represents the Arrhenius plot (ln k vs $1/T$) drawn, and the value of E_a calculated from the slope of the plot was found to be 35.15 kJmol^{-1}.

Effect of pH. The effect of pH on dye decomposition was examined over a range of pH 3–11. Because the optical spectrum remains the same in this pH range, the structure of the dye molecule probably remains unchanged. As elucidated in Figure 7, the dye decomposition is maximized at pH 3 and decreases as the pH was increased. There is a sharp decrease in dye decomposition at pH 4 when K–OMS-2 is used as a catalyst. For Mo–K–OMS-2 and K–OMS-2 with TBHP, the sharp decrease is observed beyond pH 4. The dye decomposition was not significantly altered beyond pH 9. There was, however, a slight blue shift in the λ_{max} of the dye at lower pH (3–4) values as seen in Figure S3 in the Supporting Information.

Catalyst Amount. The effect of catalyst concentration on the MB decomposition was examined using different amounts of K–OMS-2 catalyst with and without TBHP. These data are shown in Figure S4 in the Supporting Information. The percent decrease in dye was measured for the range of catalyst amounts from 12.5 to 100 mg over the 30 min course. In both cases (with and without TBHP), the catalyst amount shows a linear increase in dye-decomposing activity. These data show that the rates of these reactions are controlled by the amount of catalyst.
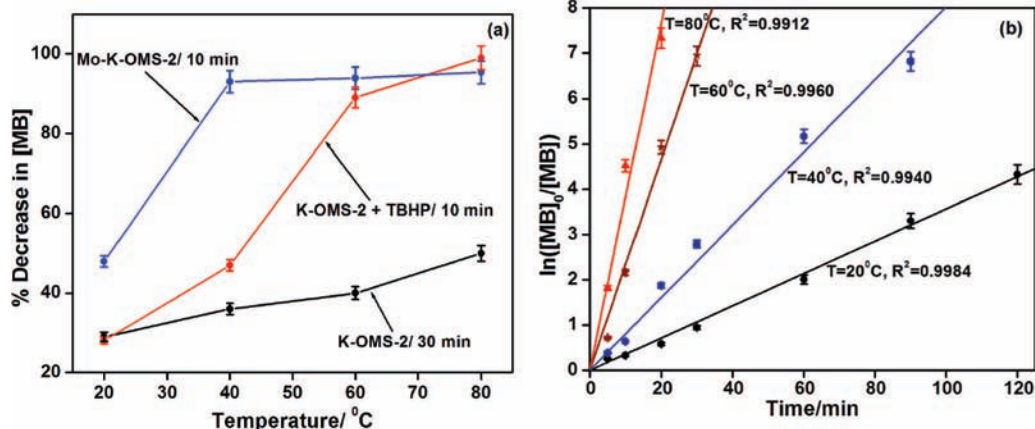
Green Decomposition of Organic Dyes

J. Phys. Chem. A, Vol. 113, No. 8, 2009 **1527**

Figure 6. (a) Percent decrease in MB dye vs temperature. Twenty-five milliliters of 120 ppm MB dye + 75 mL DDW was reacted with 50 mg of K−OMS-2 (blue) and Mo−K−OMS-2 (green). Fifty milliliters of 120 ppm MB dye was reacted with 50 mL of 0.1 M TBHP + 50 mg K−OMS-2 (red). (b) Pseudo-first-order kinetic plot of ln[MB] vs time of a 50 mL of 120 ppm dye was reacted with 50 mL of 0.1 M TBHP + 50 mg of K−OMS-2 for 120 min at different temperatures. The best fit is made for the slope for each temperature.
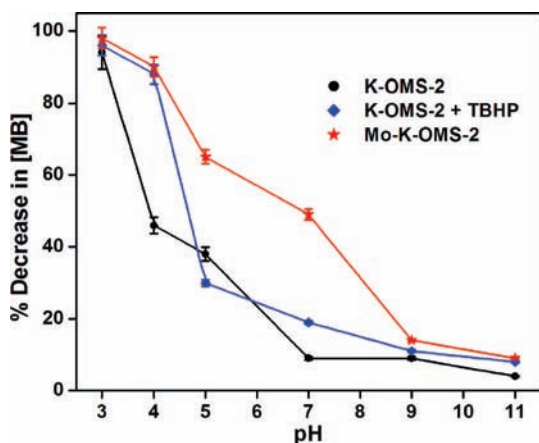

Figure 7. Percent decrease in [MB] vs pH. Twenty-five milliliters of 120 ppm MB dye in 75 mL DDW was reacted with 50 mg of K−OMS-2 (vine) and Mo−K−OMS-2 (red) for 30 min. Fifty milliliters of 120 ppm MB dye was reacted with 50 mL 0.1 M TBHP + 50 mg of K−OMS-2 for 120 min.

Figure 8. XRD patterns for K−OMS-2 before and after reaction with MB and MB+TBHP.

Structural Analysis of the Catalysts. To study the structural changes of the catalyst, powder X-ray diffraction patterns (XRD), potentiometric titrations (AOS), thermogravimetric measurements (TGA), and elemental analysis (EDX) were performed. The catalyst was recovered by filtering the reaction mixture after the reaction, and the precipitate was allowed to dry in air overnight. The XRD patterns for K−OMS-2 and K−OMS-2 with TBHP before and after reaction are compared in Figure 8. Thermogravimetric data (TGA) and elemental composition (EDX) are shown in Figures S6, S7, and S8 of the Supporting Information. AOS data done before and after reaction gave values of 3.86 and 3.85, respectively. These results suggest that no significant changes occurred in the catalyst. Similar XRD results were observed for doped Mo−K−OMS-2 catalyst before and after the reaction. Aluminum (Al) peaks were observed when the sample amount did not cover the surface of the Al sample holder.

Comparison of Catalysts. Experiments were performed to compare the dye-decomposition activity of different manganese oxide catalysts with and without TBHP. The results are tabulated in Table S1 in the Supporting Information. In the absence of TBHP, the catalysts show the activity in the range of 0−84% over 30 min time. Among all of these catalysts, AMO showed the best catalytic effect followed by K−OMS-1, Na−OL-1, and
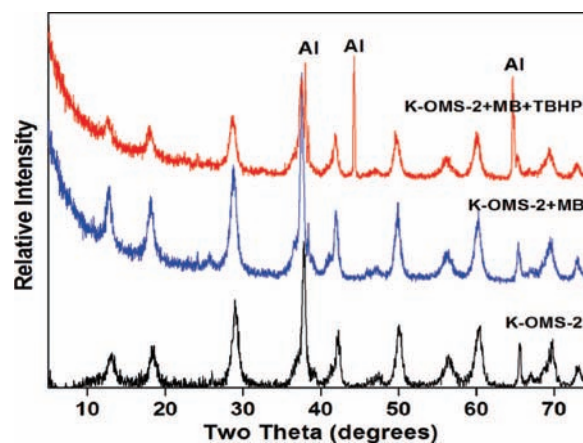
K−OMS-2, whereas commercial MnO_2 (pyrolusite) showed hardly any activity without TBHP. When TBHP was present, K−OMS-2 showed the highest activity, totally removed the dye from the solution, and AMO catalysts are a little less active. Commercial MnO_2 showed slightly increasing activity (9%), whereas K−OMS-1 and Na−OL-1 catalysts showed decreasing activity over a period of 120 min.

Products Analysis. All of the above spectrophotometric experiments showed only the total discoloration of the methylene blue dye. These results however do not show the nature of the intermediates formed during the oxidation process. Therefore, ESI-MS experiments were performed on samples collected during the course of reaction to screen the oxidized species formed during the reaction. The ESI-MS spectrum (part a of Figure 9) obtained, at 0 min of the reaction, showed only a strong signal at $m/z = 284$, corresponding to the methylene blue ion. After 30 min reaction with K−OMS-2 in the presence of TBHP, new peaks appearing at $m/z = 300$ and 316 suggest that 1 and 2 hydroxyl groups are incorporated in the aromatic ring of MB, respectively. The peaks at $m/z = 270$ and 256 are probably due to hydroxylation followed by *N*-demethylation and decarboxylation (−CO).

The spectra taken at 60 min showed that similar processes are continuing with time and suggest that cleavage of the ring structure occurs during the oxidation. The spectrum at 120 min showed some additional new peaks at lower masses ($m/z = 136$, 168, and 182), suggesting that dye decomposition occurs via
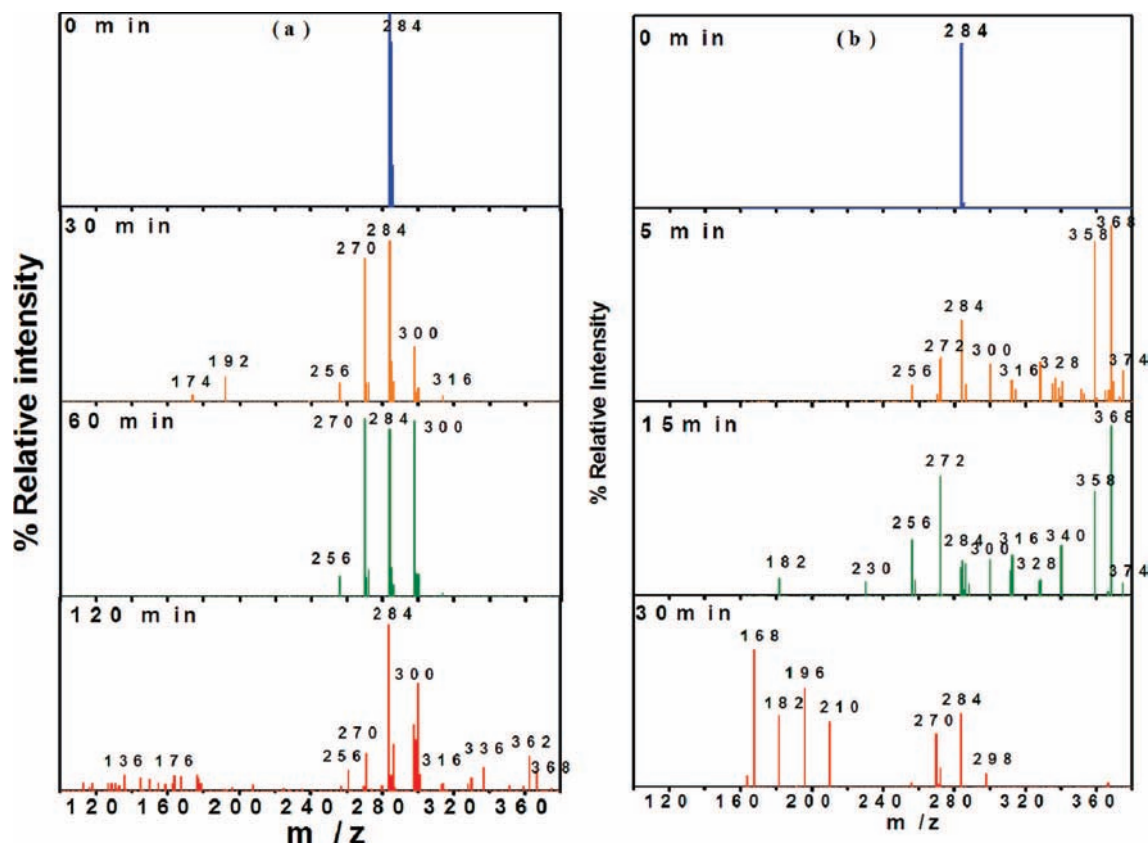
Figure 9. ESI mass spectra for monitoring the oxidation of MB (a) by K−OMS-2 + TBHP over the reaction time of 120 min, and (b) by Mo−K−OMS-2 over the time of 30 min.

degradation into smaller molecular fragments. The ESI-MS spectra taken with the collected samples after 1 week (Figure S5 of the Supporting Information) of the reaction showed no peak at $m/z = 284$, suggesting that the dye was totally decomposed to smaller fragments during this time. Similar trends were also observed when Mo−K−OMS-2 (part b of Figure 9) was used as a catalyst.

Discussion

Methylene blue (MB) has a basic dye skeleton of a thiazine group and has been classified as a toxic colorant. MB is widely used as a stain, an oxidation−reduction indicator, and has a number of biological uses. MB is known to have various harmful effects on human beings (eye irritation and lung diseases), so it is of the utmost importance to remove MB from wastewater.[2,37] There are reports where MB dye degradation has been done photochemically.[7−9] However, our experimental condition resulted in negligible photodegradation of MB even after 2 h. Experiments reported here show that MB is being oxidized by the manganese oxide catalysts.

Doped and undoped octahedral molecular sieves of manganese oxide catalysts containing transition metals are redox catalysts. They can also act as Lewis acids and therefore catalyze oxidation reactions by forming acid−base adducts[21] either with the substrate (dye molecule) or with oxidizing agents such as TBHP/H_2O_2 to enhance reactivity and act as catalysts for the decomposition reaction. TBHP and H_2O_2, oxidants considered in this study, showed totally opposite effects on dye decomposition activity with increased oxidant concentrations (part b of Figure 2). As expected, with increased concentration (0 to 0.05 M) of H_2O_2, the amount of MB dye decomposition is decreased. This similar observation was also reported by Segal[10] and

Ghosh[29] in the PC dye decomposition and liquid-phase epoxidation of olefins, respectively. The reason may be that the size of the H_2O_2 molecule is comparable to the pore size of the OMS-2 catalysts; therefore H_2O_2 can enter into the channels and decompose to water and oxygen instead of forming the catalytic active site, an oxo−metal complex. This result is in agreement with the observation that OMS-2 catalyzes the decomposition of H_2O_2 as described by Zhou et al.[38]

TBHP, a bulky oxidant (∼4.0 Å), cannot readily get into the channels and thus forms the highly reactive oxo−metal complex that helps with the decomposition of MB dye. In addition, TBHP is a stronger Lewis base than H_2O_2 because the *t*-butyl group gives a positive inductive effect on the lone pair electron of the oxygen atoms of TBHP. This can further be enhanced to form a stronger acid−base adduct between the Lewis acid sites of OMS-2 materials and Lewis base sites of TBHP. TBHP itself cannot decompose the dye, therefore causing the formation of an oxo−metal complex intermediate. The mixed-valent oxidation state of Mn (+2, +3, and +4) in OMS-2 and the transition elements (Mo^{6+}, V^{+5}, W^{6+}, Fe^{3+}, and Co^{2+}) in the doped OMS-2 are good candidates to form oxo−metal catalyst species along with TBHP. The detailed mechanism of the oxo−metal complex formation between OMS-2 and TBHP is described in the literature.[29]

Catalytic behavior of doped OMS-2 materials shows variations in their dye decomposing activities, and the differences are probably due to variations in average manganese oxidation states, dopant metal amount, oxidation states of the metals, and surface area. Surface areas of all of the materials range from ∼60 to 270 m²/g. In this study, the surface area of the catalyst follows the order of Mo > V > Fe > K > W ∼ H > Co, whereas the degree of decomposition in the presence of catalyst

Green Decomposition of Organic Dyes

J. Phys. Chem. A, Vol. 113, No. 8, 2009 **1529**

alone follows the order of Mo > V > K > H ~ W > Fe ~ Co and the catalyst with TBHP follows the order of Mo > K > V > W > H > Fe > Co. K−OMS-2 with a smaller surface area than Fe−K−OMS-2 has shown better MB degradation in both cases. A higher surface area is thus not consistent with the higher activity of all of the catalysts used. Mo−K−OMS-2 (Mo^{6+}), V−K−OMS-2 (V^{5+}), and W−K−OMS-2 (W^{6+}) showed better catalytic activity because of their d^0 metal centers forming highly reactive oxo−metal species with mono-oxygen like TBHP compared to other doped metal (Fe−K−OMS-2 (Fe^{3+}) and Co−OMS-2 (Co^{2+})) catalysts. Catalytic activity of these catalysts mainly depends on the oxidation state and the accessibility of the transition metal in the OMS-2. Other than the oxidation states, a combination of the above mentioned factors can play a role to determine the order of the activity of these catalysts. All of the doped catalysts showed enhanced activity with TBHP, showing their ability to form oxo−metal complexes that enhance reactivity.

A drastic increase in the dye decomposition activity of OMS-2 materials observed with raising temperature suggests a swelling effect produced within the internal structure of the catalyst enabling a large amount of dyes as well as TBHP molecules to penetrate through the tunnels and internal pores of the catalysts. Frequent interaction between MB dye, TBHP, and active sites of the catalyst therefore increased the decomposition of the dye. Increased activity on raising temperature implies that the enthalpy change has a positive value. This indicates that the decomposition of MB was endothermic, which opposes the argument of possible exothermic adsorption and strongly supports the oxidation of the dye by OMS-2 catalysts.

Kinetic studies show that the dye decomposition reactions by Mo−K−OMS-2 catalysts follow first-order kinetics ($k = 7.6 \times 10^{-2}$ min^{-1}), whereas K−OMS-2 along with TBHP follow pseudo-first-order kinetics ($k' = 3.6 \times 10^{-2}$ min^{-1}) with respect to dye concentration. These rate constants' values are higher than the values of 6.6×10^{-3} to 7.6×10^{-3} min^{-1} reported by S.-A. Ong et al.[41] for biodegradation of MB dye. From the rate constant, the dye decomposition reaction by K−OMS-2 + TBHP is slower when compared with only Mo−K−OMS-2 catalysts. This longer reaction suggested the formation of an oxo−catalyst species that initiates the decomposition reaction of dye in the presence of TBHP. Kinetic data obtained for the K−OMS-2 + TBHP system over various temperatures also followed pseudo-first-order kinetics. Apparent rate constants (k') have been used in obtaining an Arrhenius plot. The apparent activation energy (E_a) estimated from the slope of the plot was found to be 35.15 kJmol^{-1}.

The other important factor that significantly influences the rate of MB decomposition is pH, as seen in Figure 7. The isoelectric point (IEP) of the catalysts is important in order to keep track of the charge of the catalyst surface as a function of pH. IEP values are characteristic of the oxidation state of manganese oxides. The calculated IEPs for octahedrally coordinated Mn^{2+}, Mn^{3+}, and Mn^{4+} are 12.2, 9.6, and 5.8, respectively. The average oxidation state of Mn in OMS-2 is ~3.8−4, and consequently the IEP value for OMS-2 catalyst is ~5.8.[42] At higher pH above IEP the catalyst surface exhibits negative charge and therefore should show higher adsorption of positively charged MB molecules. Our experiments showed that lower pH favors the reaction, and as a result the interaction between MB molecules and OMS-2 catalysts is not just an electrostatic adsorption. There should be another mode of interaction that favors the oxo−metal chelation. Literature[43] data suggest that Mn is highly mobile in lower pH and its mobility

is restricted at high pH because of the high concentration of OH$^-$ ions, which can easily precipitate Mn as hydrous oxides. Observations made during the course of the reaction: The reaction rate was faster and completed in very short time at lower pH, whereas at higher pH the reaction rate was slower, decomposition is lower and saturated with time, and also in the reaction mixture dark precipitate was observed is in accordance with the above reasoning. As a result, formation of the oxo−metal complex is very fast at lower pH due to high mobility of Mn; however, at higher pH Mn easily precipitates as hydrous oxides and much less Mn is available for oxo−metal complex formation, which leads to less decomposition of MB.

The solubility of manganese oxide is exceedingly small, suggesting that the reaction is heterogeneous and must be taking place at the interface of the solid and substrate. The catalytic activity of manganese oxide may be due to excess surface oxygen and from the oxidant rather than active or available oxygen.[10,44] This is strongly supported by the XRD data that showed no changes in the bulk structure after reaction. Further analysis for elemental composition and thermogravimetric analysis for before and after reaction samples (Supporting Information) led to a similar conclusion.

Porosity and surface area are important parameters that control the differences in catalytic activity of other manganese oxide catalysts. Higher catalytic activity of AMO can be attributed to its higher surface area. Poor activity of commercial MnO_2 is in agreement with its lower surface area and porosity. The higher activity of K−OMS-1 and Na−OL-1 catalysts as compared to OMS-2 is probably ascribed to their higher pore size and pore volume, but their decreasing activity along with TBHP is a consequence of the specific selectivity of TBHP into the channels and due to decomposition rather than forming the catalytic active site an oxo−metal complex.

The decomposition follows a possible mechanism that involves formation of an oxo−metal complex of the dye molecule on the catalyst surface, oxidation (electron transfer) of dye molecule by the catalyst oxidant adduct, and then decomposition of the oxidized species. When the reaction proceeded, a decrease in the absorbance of MB at 665 nm was accompanied by a blue shift in the spectrum, with the emerging of a new absorption peak at around 400−500 nm. This indicates *N*-demethylation of MB and the formation of new intermediates.[45,46] Therefore, the ESI-MS experiments have been performed and the results are in good agreement with reports in the literature,[47,48] which show that dye decomposition is initiated through hydroxyl group incorporation in the aromatic ring followed by cleavage of dye molecules into oxidative intermediate species. This prediction was further supported by the ESI-MS spectra taken with the collected samples after 1 week of the reaction. In those spectra, there was no peak at *m/z* = 284, suggesting that the dye was totally decomposed to smaller fragments during this time. Further chemical analyses such as total organic content and HPLC-MS are clearly needed to determine the nature of the dye degradation products and also to understand processes of selective oxidation and mineralization.

Conclusions

Experimental results from this economic and environmentally friendly study show that MB dye is successfully decomposed using K−OMS-2 and doped K−OMS-2 materials. The best catalyst is Mo−K−OMS-2 because it gave a total degradation (94%) in 30 min, whereas K−OMS-2 gave only ~30% degradation. Oxidant TBHP enhanced the degree of decomposition with increasing concentration but H_2O_2 inhibited the

1530 *J. Phys. Chem. A, Vol. 113, No. 8, 2009*

Sriskandakumar et al.

reaction with increasing concentration. Rates of reaction were found to be first-order and pseudo-first-order with respect to the dye. X-ray diffraction studies indicate that negligible changes occurred in the catalyst structure after reaction. The degree of dye decomposition is increased with increasing catalyst concentration. The pH has a major role in the catalytic activity, and the best pH for these reactions is 3 or 4. A drastic increase in catalytic activity with increasing temperature implies the reaction is endothermic. AMO showed good catalytic activity for MB decomposition among other Mn oxide catalysts. Analysis of the products with ESI-MS showed that MB was successively oxidized via different intermediate species.

Supporting Information Available: Additional features illustrate: UV−vis spectra of Mo−K−OMS-2 + TBHP effect and pH effect, Arrhenius plot, different catalyst comparison study, catalytic amount effect, ESI-MS spectrum, TGA data and EDX. This material is available free of charge via the Internet at http://pubs.acs.org.

References and Notes

(1) Grabowski, E. M.; Veldhuizen, E. M.; Pemen, A. J. M.; Rutgers, W. R. *Plasma Sources Sci. Technol.* **2007**, *16*, 226.

(2) El Qada, E. N.; Allen, S. J.; Walker, G. M. *Chem. Eng. J.* **2006**, *124*, 103.

(3) Gong, R.; Zhang, X.; Liu, H.; Sun, Y.; Liu, B. *Bioresour. Technol.* **2007**, *98*, 1319.

(4) Impart, O.; Katafias, A.; Kita, P.; Mills, A.; Pietkiewicz-Graczyk, A.; Wrzeszcz, G. *Dalton Trans.* **2003**, 348.

(5) Garg, V. K.; Amita, M.; Kumar, R.; Gupta, R. *Dyes Pigm.* **2004**, *63*, 243.

(6) Ozdemir, Y.; Dogan, M.; Alkan, M. *Microporous Mesoporous Mater.* **2006**, *96*, 419.

(7) Banat, F.; Al-Asheh, S.; Al-Rawashdeh, M.; Nusair, M. *Desalination* **2005**, *181*, 225.

(8) Salem, I. A.; El-Maazawi, M. S. *Chemosphere* **2000**, *41*, 1173.

(9) Luca, V.; Osborne, M.; Sizgek, D.; Griffith, C.; Araujo, P. Z. *Chem. Mater.* **2006**, *18*, 6132.

(10) Segal, S. R.; Suib, S. L. *Chem. Mater.* **1997**, *9*, 2526.

(11) Shen, Y. F.; Zerger, R. P.; DeGuzman, R. N.; Suib, S. L.; McCurdy, L.; Potter, D.; O'Young, C. L. *Science* **1993**, *260*, 511.

(12) Brock, S. L.; Duan, N. G.; Tian, Z. R.; Giraldo, O.; Zhou, H.; Suib, S. L. *Chem. Mater.* **1998**, *10*, 2619.

(13) Shen, X.-F.; Ding, Y.-S.; Liu, J.; Cai, J.; Laubernds, K.; Zerger, R. P.; Vasiliev, A.; Aindow, M.; Suib, S. L. *Adv. Mater.* **2005**, *17*, 805.

(14) Yuan, J.; Laubernds, K.; Zhang, Q.; Suib, S. L. *J. Am. Chem. Soc.* **2003**, *125*, 4966.

(15) Ding, Y.-S.; Shen, X.-F.; Sithambaram, S.; Gomez, S.; Kumar, R.; Vincent, M. B.; Suib, S. L.; Aindow, M. *Chem. Mater.* **2005**, *17*, 5382.

(16) Villegas, J. C.; Garces, L. J.; Gomez, S.; Durand, J. P.; Suib, S. L. *Chem. Mater.* **2005**, *17*, 1910.

(17) O'Young, C. L.; Sawicki, R. A.; Suib, S. L. *Microporous Mesoporous Mater.* **1997**, *11*, 1.

(18) Shen, X.-F.; Ding, Y.-S.; Liu, J.; Laubernds, K.; Zerger, R. P.; Polverejan, M.; Son, Y.-C.; Aindow, M.; Suib, S. L. *Chem. Mater.* **2004**, *16*, 5327.

(19) Yin, Y. G.; Xu, W. Q.; DeGuzman, R. N.; Suib, S. L.; O'Young, C. L. *Inorg. Chem.* **1994**, *33*, 4384.

(20) Duan, N. G.; Suib, S. L.; O'Young, C. L. *J. Chem. Soc., Chem. Commun.* **1995**, *13*, 1367.

(21) Ghosh, R.; Shen, X. F.; Villegas, J. C.; Ding, Y.; Malinger, K.; Suib, S. L. *J. Phys. Chem. B* **2006**, *110* (14), 7592.

(22) Krishnan, V. V.; Suib, S. L. *J. Catal.* **1999**, *184*, 305.

(23) Wang, J. Y.; Xia, G.-G.; Yin, Y. G.; Suib, S. L.; O'Young, C. L. *J. Catal.* **1998**, *176*, 275.

(24) Son, Y.-C.; Makwana, V. D.; Howell, A. R.; Suib, S. L. *Angew. Chem., Int. Ed.* **2002**, *40* (22), 4280.

(25) Malinger, K. A.; Laubernds, K.; Son, Y.-C.; Suib, S. L. *Chem. Mater.* **2004**, *16*, 4296.

(26) Opembe, N. N.; Son, Y.-C.; Sriskandakumar, T.; Suib, S. L. *ChemSusChem* **2008**, *1* (3), 182–185.

(27) Zhou, H.; Suib, S. L.; Chen, X. ; Wang, J. Y.; Luo, J.; Xia, G.-G. *Book of Abstracts*, 218th National Meeting of the American Chemical Society, New Orleans, LA, Aug 22−26, 1999; American Chemical Society: Washington, DC, 1999.

(28) (a) O'Young, C. L.; Sawicki, R. A.; Yin, Y. G.; Xu, W. Q.; Suib, S. L. Dehydration of n-parrafins to n-olefins Employing Manganese Oxide Octahedral Molecular Sieve as a Catalyst. Patent 5,597,944, 1997. (b) Wang, J. Y.; Xia, G.-G.; Yin, Y. G.; Suib, S. L. *Chem. Ind.* **1998**, *75*, 621.

(29) Ghosh, R.; Son, Y.-C.; Makwana, V. D.; Suib, S. L. *J. Catal.* **2004**, *224*, 288.

(30) Kumar, R.; Garces, L. J.; Son, Y.-C.; Suib, S. L.; Malz, R. E., Jr. *J. Catal.* **2005**, *236*, 387.

(31) Li, W.-N.; Yuan, J.; Gomez, S.; Sithambaram, S.; Suib, S. L. *J. Phys. Chem. B* **2006**, *110*, 3066.

(32) Malinger, K. A.; Ding, Y.-S.; Sithambaram, S.; Espinal, L.; Gomez, S.; Suib, S. L. *J. Catal.* **2006**, *239*, 290.

(33) Makwana, V. D.; Son, Y.-C.; Howell, A. R.; Suib, S. L. *J. Catal.* **2002**, *210*, 46.

(34) Shen, Y. F.; Suib, S. L.; O'Young, C. L. *J. Am. Chem. Soc.* **1994**, *116* (24), 11020.

(35) Suib, S. L. In Recent Advancements and New Horizons in Zeolite Science and Technology. *Stud. Surf. Sci. Catal.* **1996**, *102*, 47.

(36) Pavan, F. A.; Gushikem, Y.; Mazzocato, A. C.; Dias, S. L. P.; Lima, E. C. *Dyes Pigm.* **2007**, *72*, 256.

(37) Hamdaoui, O. *J. Hazard. Mater.* **2006**, *B135*, 264.

(38) Zhou, H.; Shen, Y. F.; Wang, J. Y.; Chen, X.; O'Young, C. L.; Suib, S. L. *J. Catal.* **1998**, *176*, 321.

(39) Sheldon, R. A.; Go, I. W. C. E.; Lempers, H. E. B. *Catal. Today* **1998**, *41*, 387–407.

(40) Srukul, G. *Catalytic Oxidation with Hydrogen Peroxide as Oxidant*; Strukul, G., Ed.; Kluwer: Dordrecht, The Netherlands, 1992; pp 1−11.

(41) Ong, S.-A.; Toorisaka, E.; Hirata, M.; Hano, T. *J. Hazard. Mater.* **2005**, *B124*, 88.

(42) Morimoto, T.; Kittaka, S. *Bull. Chem. Soc. Jpn.* **1974**, *47* (7), 1586.

(43) Post, J. E. *Proc. Natl. Acad. Sci. U.S.A.* **1999**, *96*, 3447.

(44) Kanungo, S. B.; Parida, K. M.; Sant, B. R. *Electrochim. Acta* **1981**, *26* (8), 1157.

(45) Li, J.; Ma, W.; Huang, Y.; Cheng, M.; Zhao, J.; Yu, J. C. *Chem. Commun.* **2003**, 2214.

(46) Donaldson, J. D.; Grimes, S. M.; Yasri, N. G.; Wheals, B.; Parrick, J.; Errington, W. E. *J. Chem. Technol. Biotechnol.* **2002**, *77*, 756.

(47) Oliveira, L. C. A.; Goncalves, M.; Guerreiro, M. C.; Ramalho, T. C.; Fabris, J. D.; Pereira, M. C.; Sapag, K. *Appl. Catal., A* **2007**, *316*, 117.

(48) Chen, F.; Ma, W.; He, J.; Zhao, J. *J. Phys. Chem. A* **2002**, *106*, 9485.